Computer Assisted Mechanics and Engineering Sciences, 14: 471–484, 2007.

Thermal radiation effects on hydromagnetic flow

Mohamed M. Abdelkhalek
Atomic Energy Authority, Nuclear Research Centre, Nuclear Physics Department
Cairo, Egypt

(Received October 12, 2005)

Numerical results are presented for the effects of thermal radiation, buoyancy and heat generation or absorption on hydromagnetic flow over an accelerating permeable surface. These results are obtained by solving the coupled nonlinear partial differential equations describing the conservation of mass, momentum and energy by a perturbation technique. This qualitatively agrees with the expectations, since the magnetic field exerts a retarding force on the free convection flow. A parametric study is performed to illustrate the influence of the radiation parameter, magnetic parameter, Prandtl number, Grashof number and Schmidt number on the profiles of the velocity components and temperature. The effects of the different parameters on the velocity and temperature profiles as well as the skin friction and wall heat transfer are presented graphically. Favorable comparisons with previously published work confirm the correctness of numerical results.

Keywords: heat and mass transfer, hydromagnetic flow, perturbation technique

1. Introduction

The study of the dynamics of conducting fluid find applications in a variety of engineering problems, the one related to the cooling processes of nuclear reactors, and that related to the connected flow through a porous medium, since the geothermic region gases are electrically conducting and affected by a magnetic field. The effect radiation MHD flow and heat transfer problems have become more important industrially. At high operating temperature, radiation effect can be quite significant. Many processes in engineering areas occur at high temperatures and knowledge of radiation heat transfer becomes very important for the design of pertinent equipment. Nuclear power plants, gas turbines and the various propulsion devices for aircraft, missiles, satellites and space vehicles are examples of such engineering areas. In recent years, considerable progress has been made in the study of heat and mass transfer in magnetohydrodynamics flow due to its application in many devices, like the MHD power generator and Hall accelerator. The influence of a magnetic field on the flow of an electrically conducting viscous fluid with mass transfer and radiation absorption is also useful in planetary atmosphere research [1].

Ram *et al.* [2] studied the heat and mass transfer of a viscous heat generating fluid with hall current. Jha and Prasad [3] investigated MHD free convection and mass transfer flow through a porous medium with heat source. Takhar *et al.* [4] investigated the hydromagnetic convection flow of a heat generating fluid past a vertical plate with hall current and heat flux through a porous medium. Georgiou and Georgantpoulos [5] studied the mass transfer effects on the transient behavior of the asymptotic laminar boundary layer. Hydromagnetic flows and heat transfer have become more important in recent years because of many important applications, for example in many metallurgical processes which involve cooling of continuous strips or filaments, these elements are drawn through a quiescent fluid. During this process, these strips are sometimes stretched. The properties of the final product depend to a great extent on the rate of cooling. This rate of cooling has been proven to be controlled and, therefore, the quality of the final product by drawing such strips in an electrically conducting fluid subject to a magnetic field [9]. Soundalgekar *et al.* [6] used a finite difference method to investigate free convection effects on the Stokes problem for a vertical plate in a dissipative fluid with constant heat flux.

Ram [7] also used the finite difference method to solve the MHD Stokes problem for vertical plate with hall and ion slip currents. Chaturvedi [8] studied the flow of incompressible viscous fluid past an impulsively started infinite porous plate with variable suction. Many works have been reported on flow and heat transfer over a stretched surface in the presence of a magnetic field [9–20]. Takhar *et al.* [21] studied the radiation effects on MHD free-convection flow of a gas past a semi-infinite vertical plate. Recently the radiation effect on heat transfer over a stretching surface was studied by Elbashbeshy [22].

The purpose of this work is to study the effect of thermal radiation and heat generation or absorption on hydromagnetic flow over an accelerating permeable surface. The coupled nonlinear partial differential equations are solved by the perturbation technique. The effects of the different parameters on the velocity and temperature profiles as well as the skin friction and wall heat transfer are presented graphically.

2. Formulation of the Problem

Consider steady, laminar, viscous boundary-layer flow over an accelerating semi-infinite vertical permeable surface. A uniform magnetic field is applied in the horizontal direction that is normal to the surface. A temperature dependent heat source or sink is assumed to be present in the flow and that thermal radiation and buoyancy effects are significant. All fluid properties are assumed to be constant except the density in the body force term of the balance of linear momentum. The magnetic Reynolds number is assumed to be small so that the induced magnetic field is neglected. No electric field is assumed to exist and both viscous and magnetic dissipations are neglected. Under these assumptions, along with Boussinesq approximations, the boundary layer equations for this problem can be written as [12]

$$\frac{\partial u}{\partial x}+\frac{\partial v}{\partial y}=0, \tag{1}$$

$$u\frac{\partial u}{\partial x}+v\frac{\partial u}{\partial y}=\nu\frac{\partial^2 u}{\partial y^2}+g\,\beta(T-T_\infty)-\frac{\sigma B_0^2}{\rho}u, \tag{2}$$

$$u\frac{\partial T}{\partial x}+v\frac{\partial T}{\partial y}=\alpha\frac{\partial^2 T}{\partial y^2}+\frac{\beta^* u}{\rho C_P}(T_\infty-T)+\frac{Q_0}{\rho C_P}(T-T_\infty)-\frac{1}{\rho C_P}\frac{\partial q_r}{\partial y}, \tag{3}$$

where x, y are the vertical and horizontal directions, respectively, u, v and T are the fluid velocity component in the x and y directions and temperature, respectively, ρ is the fluid density, ν is the kinematic viscosity, C_P is specific heat at constant pressure, $\alpha(K_t/\rho C_P)$ is the thermal diffusivity, K_t is the fluid thermal conductivity, β is the volumetric expansion coefficient, β^* is a constant, Q_0 is a constant, σ is the electric conductivity, B_0 is applied magnetic induction, g is the gravitational acceleration. The terms $\beta^* u(T_\infty - T)$ and $Q_0(T - T_\infty)$, (with β^* and Q_0 being constants) both represent the heat generated or absorbed per unit volume. The first form was used by Acharya *et al.* [23] while the last form was used by Vajravelu and Nayfeh [26] and Chamkha [12, 27] . The reason for retaining both forms in the present work will be explained below, q_r is the thermal radiation and T_∞ is the free stream temperature. The radiative heat flux term q_r is simplified by using the Rosseland approximation (see [12, 16, 24, 25]).

$$q_r=-\frac{4\sigma^*}{3K^*}\frac{\partial T^4}{\partial y} \tag{4}$$

where σ^* and K^* are the Stefan–Boltzmann constant and the mean absorption coefficient, respectively.

The fluid phase temperature differences within the flow are assumed to be sufficiently small so that T^4 may be expressed as a linear function of temperature. This is done by expanding T^4 in a Taylor series about the free stream temperature T_∞ and neglecting higher-order terms to yield

$$T^4 = 4T_\infty^3 T - 3T_\infty^4 .$$

By employing Eq. (4), Eq. (2) becomes

$$u\frac{\partial T}{\partial x} + v\frac{\partial T}{\partial y} = \alpha\frac{\partial^2 T}{\partial y^2} + \frac{\beta^* u}{\rho C_P}(T_\infty - T) + \frac{Q_0}{\rho C_P}(T - T_\infty) + \frac{16a^* T_\infty^3}{3\rho C_P K^*}\frac{\partial^2 T}{\partial y^2} \tag{5}$$

and the boundary conditions can be written as

$$\begin{aligned} &u(x,0) = ax, \quad v(x,0) = v_w, \qquad T(x,0) = T_w(x) = T_\infty + A_0 x, \\ &u(x,\infty) = 0, \quad T(x,\infty) = T_\infty, \end{aligned} \tag{6}$$

where a is a constant, v_w is the wall suction ($v_w < 0$) or injection ($v_w > 0$) velocity, and $T_w(x)$ is the wall temperature.

Using the stream function ψ such that

$$u = \frac{\partial \psi}{\partial y}, \quad v = -\frac{\partial \psi}{\partial x}, \tag{7}$$

and substituting the following non-dimensional similarity transformation

$$\psi = \sqrt{\nu a}\, x f(\eta), \qquad \eta = \sqrt{\frac{a}{\nu}}\, y, \qquad \theta = \frac{T - T_\infty}{T_w - T_\infty}. \tag{8}$$

By substitution Eqs. (7)–(8) into Eqs. (1)–(3), we get

$$f''' + ff'' - (f' - M^2)f' = -G_r\theta, \tag{9}$$

$$\frac{(N_R+1)}{P_r}\theta'' + f\theta' - (1+\delta_x)f'\theta = -\Delta\theta, \tag{10}$$

where the Hartmann number $M = \left(\frac{\sigma}{\rho a}\right)^{0.5} B_0$, the Grashof number $G_r = \frac{g\beta(T_w - T_\infty)}{a^2 x}$, the Prandtl number $P_r = \frac{\nu}{\alpha}$, the thermal radiation parameter $N_R = \frac{16\sigma^* T_\infty^3}{3K^* K_t}$, $\delta_x = \frac{\beta^* x}{\rho C_P}$ – heat generation, $\Delta = \frac{Q_0}{\rho C_P \alpha}$ – heat absorption.

It is seen from $\delta_x = \frac{\beta^* x}{\rho C_P}$ and $\Delta = \frac{Q_0}{\rho C_P \alpha}$ that using a heat generation or absorption effect of the form $\beta^* u(T_\infty - T)$ produces a locally similar set of equations since δ_x depends on x. However, by employing the form $Q_0(T - T_\infty)$ yields self-similar equations everywhere along the surface. Since one of the objectives of this work is to obtain similarity equations, the second form for the heat generation or absorption effect is employed. Also, the first form is kept in the formulation for merely comparison purposes with [12, 23]. It should be noted here that positive values of Δ indicate heat generation while negative values of Δ indicate heat absorption.

The appropriate flat plate, free convection boundary condition is also transformed into the applicable form

$$\begin{aligned} &f'(0) = 1, \quad f(0) = -f_0, \quad \theta(0) = 1, \\ &f'(\infty) = 0, \quad \theta(\infty) = 0, \end{aligned} \tag{11}$$

where $f_0 = \frac{v_w}{\sqrt{a\nu}}$ is the wall mass transfer coefficient such that $f_0 < 0$ indicates wall suction and $f_0 > 0$ corresponds to wall blowing conditions.

The resulting differential equations contain arbitrary parameters, the Prandtl number P_r, the magnetic field strength and the buoyant force, the ratio of the Hartmann number is a measure of the relative influence of the magnetic and buoyant forces on the temperature and flow fields. Solution of the resulting semi-infinite domain, nonlinear equations is accomplished with a three part series method. The employed power series, contains a term A that satisfies the boundary conditions and differential equations at infinity, a second term that satisfies the boundary conditions at zero and is the solution to the initial homogeneous differential equation, and additional terms that are utilized to obtain increased numerical accuracy. This accuracy is limited by number of terms that will not initiate divergence of the numerical results,

$$F = A + \varepsilon F_1 + \varepsilon^2 F_2 + \varepsilon^3 F_3 + \cdots \tag{12}$$

$$\theta = \varepsilon\theta_1 + \varepsilon^2\theta_2 + \varepsilon^3\theta_3 + \cdots \tag{13}$$

$$\begin{aligned} &\eta = 0, \qquad F'(0) = 1, \quad F_1(0) = -F_0, \quad F_2(0) = F_3(0) = 0, \\ &\qquad\qquad \theta_1(0) = 1, \quad \theta_2(0) = \theta_3(0) = 0 \\ &\eta \to \infty, \quad F_n'(\infty) = F_n(\infty) = 0, \quad F(\infty) = A, \quad \theta_n(\infty) = 0, \quad n = 1, 2, 3, \end{aligned} \tag{14}$$

Equation (13), the temperature representation, along with Eq. (12) and the associated boundary conditions Eq. (14), contain an undetermined parameter $\varepsilon \ll 1$ which aids in the collection of terms for each set of the resulting linear differential equations. Substitution of the series representation into the differential equations and collection of terms by like powers of ε result in a family of linear differential equations, and the first three sets are

$$F_1''' + AF_1''' - M^2 F_1' = -G_r\theta_1, \tag{15}$$

$$\frac{(N_R+1)}{P_r}\theta_1'' + A\theta_1' + \Delta\theta_1 = 0. \tag{16}$$

$$F_2''' + AF_2'' - M^2 F_2' = -F_1 F_1''' + F_1'^2 - G_r\theta_2, \tag{17}$$

$$\frac{(N_R+1)}{P_r}\theta_2'' + A\theta_2' + \Delta\theta_2 = -F_1\theta_1' + (1+\delta_x)F_1'\theta_1, \tag{18}$$

$$F_3''' + AF_3'' - M^2 F_3' = -F_1 F_2'' - F_2 F_1'' + 2F_1'F_2' - G_r\theta_3, \tag{19}$$

$$\frac{(N_R+1)}{P_r}\theta_3'' + A\theta_3' + \Delta\theta_3 = -F_1\theta_2' - F_2\theta_1' + (1+\delta_x)(F_1'\theta_2 + F_2'\theta_1). \tag{20}$$

The solutions to the first two sets, Eqs. (21)–(23), when substituted into Eqs. (12)–(13), provide the required representations for F and θ'. The constant A is determined by satisfying the boundary conditions $F(0)$ and is a function of P_r and M,

$$\theta_1 = e^{-a_1\eta}, \tag{21}$$

$$F_1 = -f_0 + a_3(e^{a_2\eta} - 1) + \frac{G_r(e^{-a_1\eta} - 1)}{a_1(a_1^2 - Aa_1 - M^2)}, \tag{22}$$

$$\theta_2 = -(a_5 + a_6)e^{-a_1\eta} + a_5 e^{(a_2 - a_1)\eta} + a_6 e^{-2a_1\eta} + a_7\eta e^{-a_1\eta}, \tag{23}$$

$$F_2 = a_{18} + (a_{17} + a_{92}\eta)e^{a_2\eta} - (a_{13} + a_{16} + a_{94} + a_{93}\eta)e^{-a_1\eta} - a_{14}e^{(a_2 - a_1)\eta} + a_{15}e^{-2a_1\eta}. \tag{24}$$

The coefficients a_i are specified in the Appendix.

It should be mentioned that the skin friction coefficient and the wall heat transfer are important physical parameters for this flow and heat transfer situation. Knowing the velocity, we can calculate the skin friction and from temperature field, the rate of heat transfer in terms of the Nusselt number. These parameters can be defined as follows,

$$C_f = \frac{\mu\,(\partial u/\partial y)\,(x,0)}{\mu\,(a/\nu)^{0.5}\;ax} = f''(0),$$

$$Q = \frac{-K\,(\partial T/\partial y)\,(x,0)}{K\,(a/\nu)^{0.5}\,(T_w - T_\infty)} = -\theta'(0).$$

It is seen that C_f and Q are directly proportional to the wall velocity and temperature gradients, respectively.

3. Results and Discussions

For the purpose of discussing the results, some numerical calculations are carried out for non-dimensional velocity, surface temperature gradient, skin friction and Nusselt number for different values of heat generation, wall suction/blowing conditions, Grashof number, Hartmann number, thermal radiation parameter and heat absorption generation. In order to verify the accuracy of our present method, a comparison of non-dimensional wall velocity gradient $f''(0)$ and Nusselt number $(-\theta'(0))$, with those reported previously by Acharya *et al.* [23] and Chamkha [12]. The result of this comparison is given in Table 1. The comparisons in all the above cases are found to be in excellent agreement. Sets of representative numerical results are illustrated graphically.

Table 1. Comparison of the non-dimensional wall temperature gradient $(-\theta'(0))$

	$f_0 = 0.45$, $\delta_x = 0.5$	$f_0 = 0.45$, $\delta_x = 1.0$	$f_0 = 0.0$, $\delta_x = 0.5$	$f_0 = 0.0$, $\delta_x = 1.0$
Acharya *et al.* [23]	0.8225	0.9618	0.9462	1.0789
Chamkha [12]	0.82397	0.96191	0.94769	1.07996
Present work	0.822757	0.9626045	0.946481	1.077021

Figures 1 and 2 illustrate the non dimensional wall temperature gradient $(-\theta'(0))$ against magnetic parameter M for several of the heat generation or absorption parameter δ_x and the suction/injection parameter f_0 values. It is known that imposition of wall fluid suction reduces both the hydrodynamic and thermal boundary layers, which indicate reduction in both fluid velocity and temperature profiles. However, the exact opposite behavior is produced by imposition of wall fluid blowing or injection. Figs 1 and 2 show that the non-dimensional wall temperature gradient $(-\theta'(0))$ increases as δ_x increases.

Figures 3 and 4 illustrate the variations of the wall velocity $(-f''(0))$ against magnetic parameter M for various values of suction / injection f_0 and the thermal Radiation parameter N_R. As mentioned before increasing the value of the suction / injection parameter f_0 causes both the hydrodynamic and thermal boundary layers to increase causing the wall gradients of both the velocity and temperature profiles to decrease.

To see the effect of Grashof number (G_r) on the boundary layer flow, in Figs. 5 and 6, the non-dimensional velocity $f'(\eta)$ and the non-dimensional temperature $\theta(\eta)$ are plotted against η for different values of (G_r), respectively. All other parameters are set to zero in order to study the influence of a single effect at a time. Increase of Grashof number has the tendency of inducing more flow in the boundary layer due to the effect of the thermal buoyancy. For small buoyancy effects $(G_r = 1.0)$, the maximum flow velocity occurs at the surface. However, as the buoyancy effect becomes relatively large, a distinctive peak in the velocity profile occurs in the fluid adjacent to the wall and this peak becomes more distinctive as (G_r) increases further. Along with this flow behavior, the thermal boundary layer reduces as (G_r) increases causing the fluid temperature to reduce at every point other than that of the wall. It can be seen from Figs. 5 and 6 that as expected, f' increases but θ decreases with increasing Grashof number (G_r). In addition, the curves show that the peak value of velocity increases rapidly near the wall of the plate as Grashof number increases, and then decays to the relevant free stream velocity.

Figures 7 and 8 display the variation of velocity $f'(\eta)$ and temperature $\theta(\eta)$ for several values of magnetic parameter (M). Application of a transverse magnetic field to an electrically conducting fluid gives rise to a resistive type force called the Lorentz force, which opposes the flow, also increases and leads to enhanced deceleration of the flow. The result qualitatively agrees with expectations,

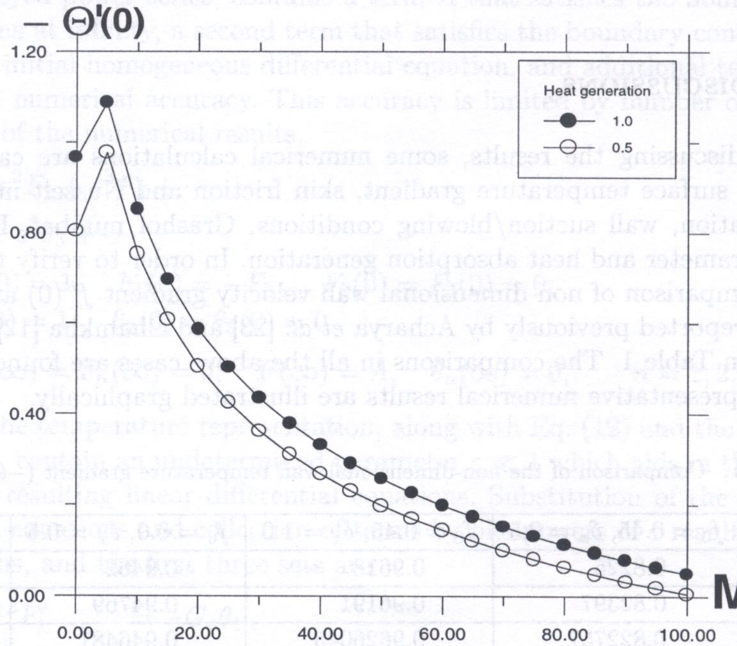

Fig. 1. Variation of non-dimensional wall temperature gradient $(-\theta'(0))$, for different values of heat generation δ_x , when $P_r = 0.71$, $G_r = 0.0$, $f_0 = 0.45$, $N_R = 0.0$, $\Delta = 0.0$, $\eta = 1.0$

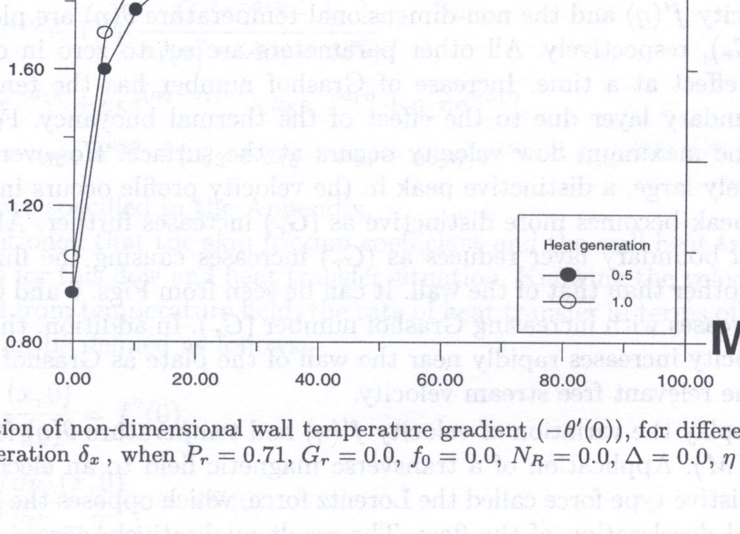

Fig. 2. Variation of non-dimensional wall temperature gradient $(-\theta'(0))$, for different values of heat generation δ_x , when $P_r = 0.71$, $G_r = 0.0$, $f_0 = 0.0$, $N_R = 0.0$, $\Delta = 0.0$, $\eta = 1.0$

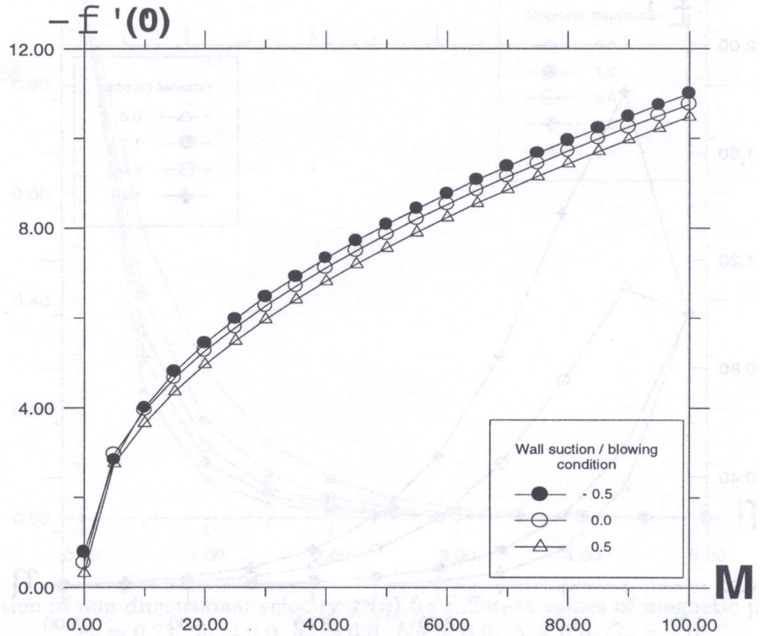

Fig. 3. Variation of non dimensional surface velocity gradient $(-f''(0))$, for different values of wall suction blowing (f_0), when $P_r = 0.71$, $G_r = 1.0$, $\delta_x = 0.0$, $N_R = 0.0$, $\Delta = 0.0$, $\eta = 1.0$

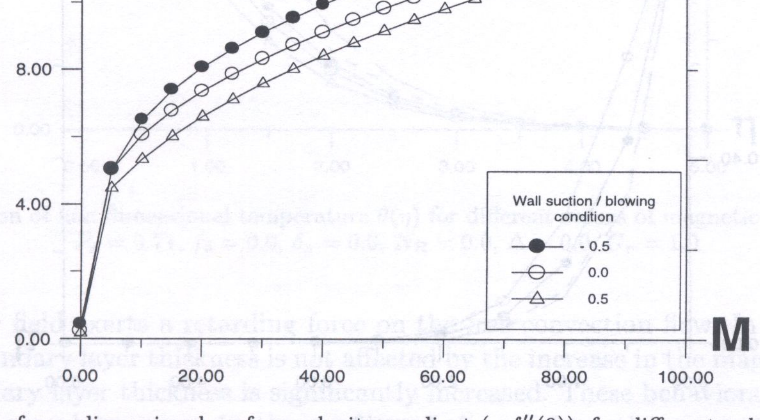

Fig. 4. Variation of non dimensional surface velocity gradient $(-f''(0))$, for different values of wall suction blowing (f_0), when $P_r = 0.71$, $G_r = 1.0$, $\delta_x = 0.0$, $N_R = 5.0$, $\Delta = 0.0$, $\eta = 1.0$

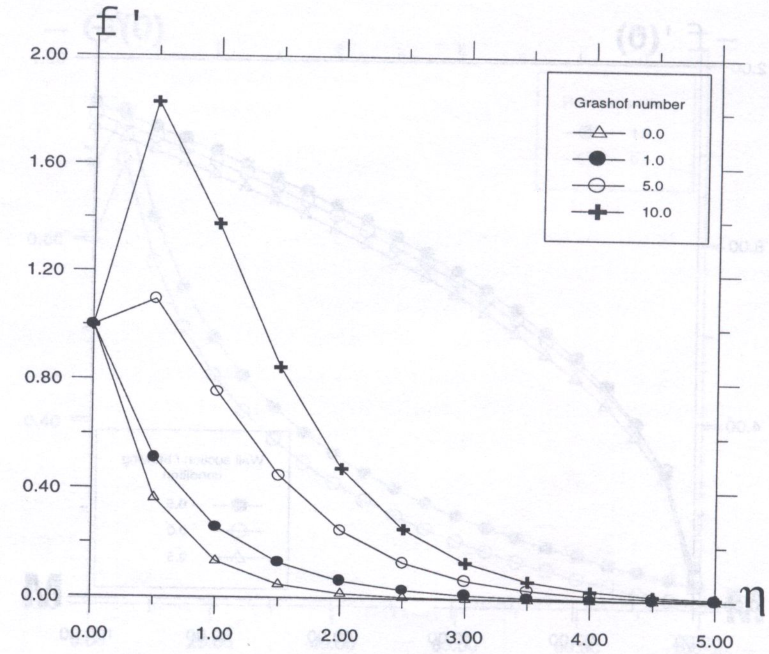

Fig. 5. Variation of non dimensional velocity $f'(\eta)$ for different values of Grashof number (G_r) when $P_r = 0.71$, $f_0 = 0.0$, $\delta_x = 0.0$, $N_R = 5.0$, $\Delta = 0.0$, $M = 0.0$

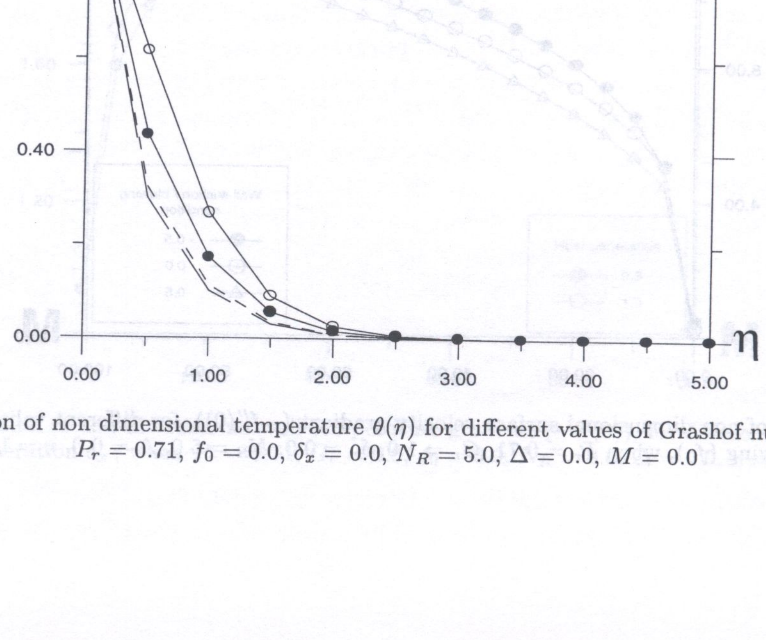

Fig. 6. Variation of non dimensional temperature $\theta(\eta)$ for different values of Grashof number (G_r) when $P_r = 0.71$, $f_0 = 0.0$, $\delta_x = 0.0$, $N_R = 5.0$, $\Delta = 0.0$, $M = 0.0$

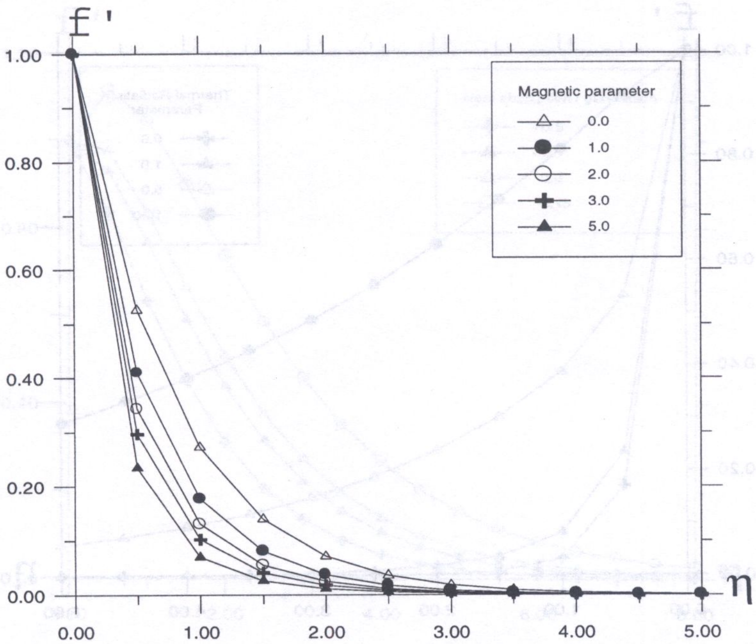

Fig. 7. Variation of non dimensional velocity $f'(\eta)$ for different values of magnetic parameter, when $P_r = 0.71$, $f_0 = 0.0$, $\delta_x = 0.0$, $N_R = 0.0$, $\Delta = 0.0$, $G_r = 1.0$

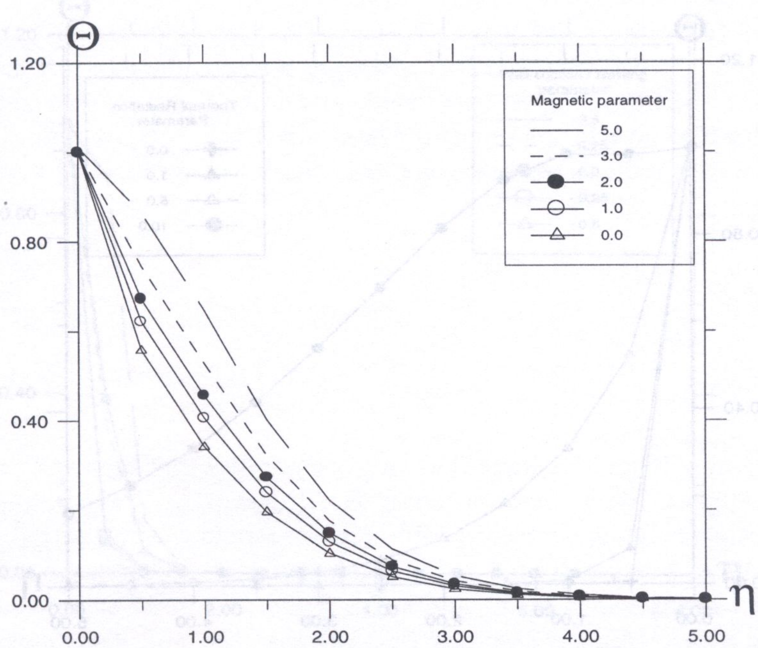

Fig. 8. Variation of non dimensional temperature $\theta(\eta)$ for different values of magnetic parameter, when $P_r = 0.71$, $f_0 = 0.0$, $\delta_x = 0.0$, $N_R = 0.0$, $\Delta = 0.0$, $G_r = 1.0$

since the magnetic field exerts a retarding force on the free convection flow. In addition, while the hydrodynamic boundary layer thickness is not affected by the increase in the magnetic field strength, the thermal boundary layer thickness is significantly increased. These behaviors are depicted in the respective decreases and increases in the profiles of f' and θ as the magnetic parameter M is increased. This means that the magnetic field works to increase the values of the temperature in the flow field and then decreases the gradient at the wall and increases thickness of the thermal boundary layer.

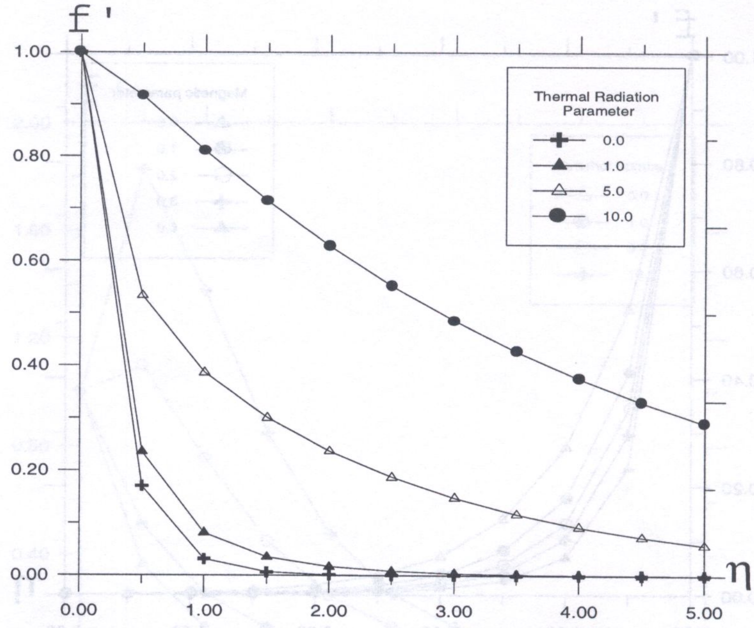

Fig. 9. Variation of non dimensional velocity $f'(\eta)$ for different values of thermal radiation parameter, when $P_r = 0.71$, $f_0 = 0.0$, $\delta_x = 0.0$, $N_R = 0.0$, $\Delta = 0.0$, $G_r = 1.0$

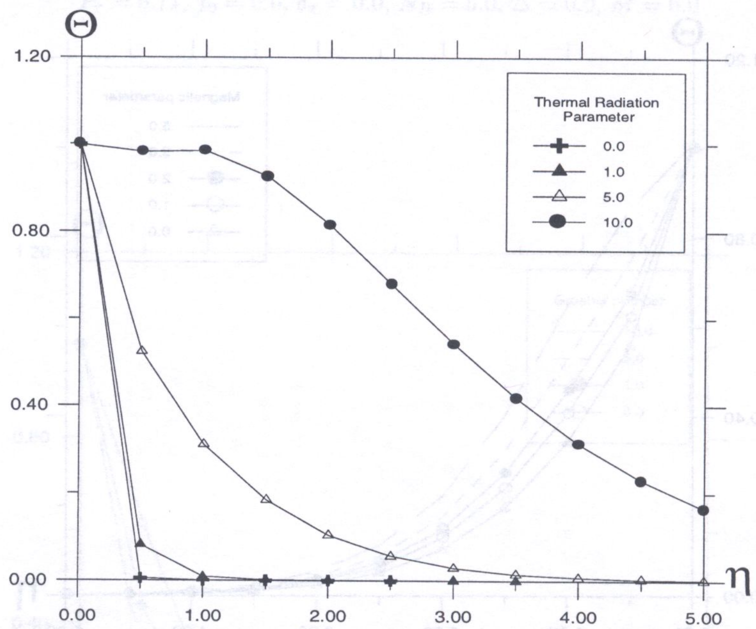

Fig. 10. Variation of non dimensional temperature $\theta(\eta)$ for different values of thermal radiation parameter, when $P_r = 0.71$, $f_0 = 0.0$, $\delta_x = 0.0$, $N_R = 0.0$, $\Delta = 0.0$, $G_r = 1.0$

Figures 9 and 10 are the graphical representation of horizontal velocity profile $f'(\eta)$ and temperature profile $\theta(\eta)$ against η for different values of the thermal radiation parameter N_R, respectively. The radiation have significant influences on velocity profiles, temperature profiles. It is observed here that the radiation have significant influences on velocity profiles, temperature profiles. Increasing the thermal radiation parameter N_R gives a significant increases in the thermal condition of the fluid and its thermal boundary layer. Through the buoyancy effect, this increase in the fluid temperature induces more flow in the boundary layer causing the higher velocity of the fluid there. In addition,

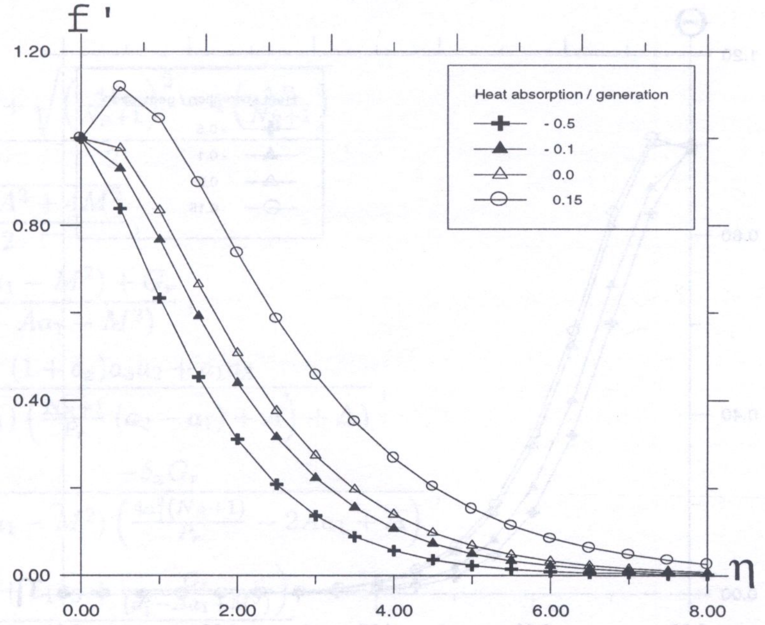

Fig. 11. Variation of non dimensional velocity $f'(\eta)$ for different values of heat absorption/generation parameter, when $P_r = 0.71$, $f_0 = 0.0$, $\delta_x = 0.0$, $N_R = 0.0$, $\Delta = 0.0$, $G_r = 1.0$, $M = 0.0$

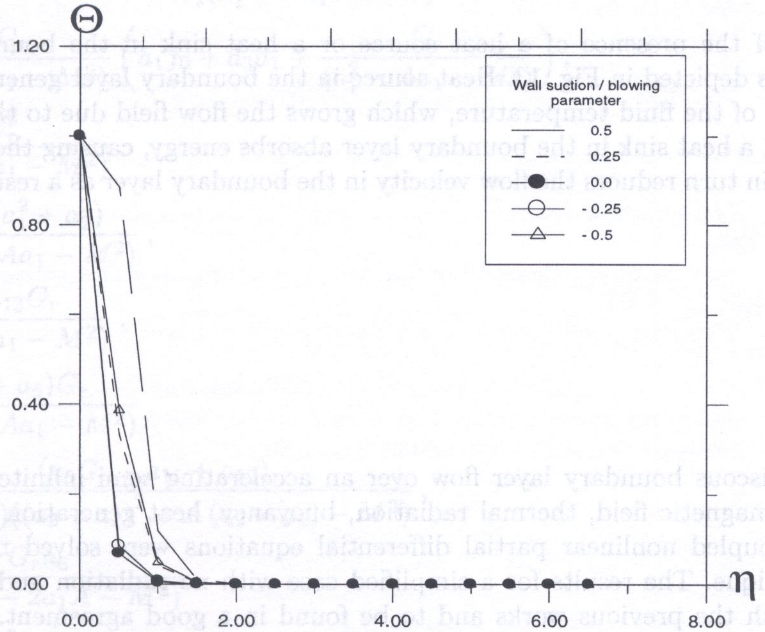

Fig. 12. Variation of non dimensional temperature $\theta(\eta)$ for different values of wall suction/blowing parameter, when $P_r = 0.71$, $f_0 = 0.0$, $\delta_x = 0.0$, $N_R = 0.0$, $\Delta = 0.0$, $G_r = 1.0$, $M = 0.0$

the hydrodynamic boundary layer thickness grows with N_R. These behaviors are clearly shown in Figs. 9 and 10.

The effect of surface mass transfer f_0 on the dimensionless velocity and temperature distributions is displayed in Figs. 11 and 12. Suction makes the velocity and temperature distributions more uniform within the boundary layer. It is known that wall fluid suction reduces both the hydrodynamic and thermal boundary layers, which indicate reduction in both the fluid velocity and temperature profiles. However, the exact opposite behavior is observed by the imposition of wall fluid blowing or injection. These behaviors are clear from Figs. 11 and 12.

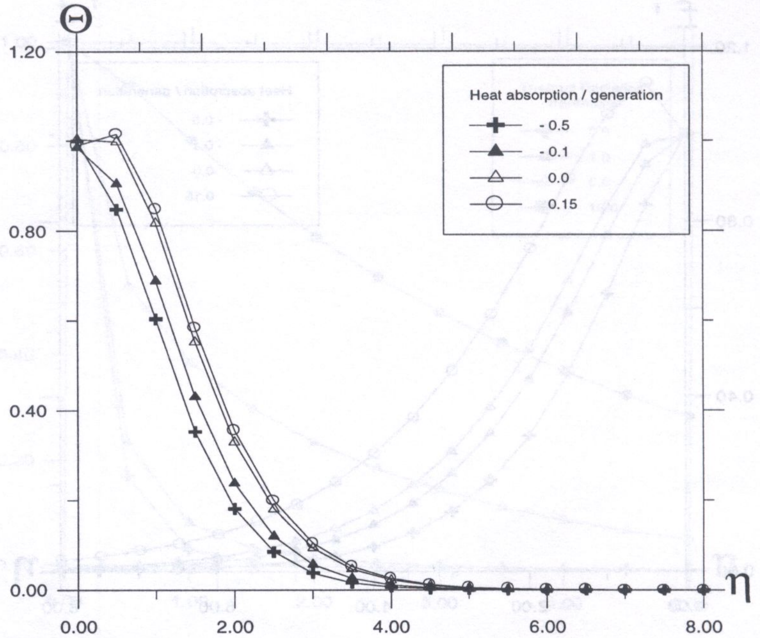

Fig. 13. Variation of non dimensional temperature $\theta(\eta)$ for different values of heat absorption/generation parameter, when $P_r = 0.71$, $f_0 = 0.0$, $\delta_x = 0.0$, $N_R = 0.0$, $\Delta = 0.0$, $G_r = 1.0$, $M = 0.0$

The influence of the presence of a heat source or a heat sink in the boundary layer on the temperature field is depicted in Fig. 13. Heat source in the boundary layer generates energy, which causes the increase of the fluid temperature, which grows the flow field due to the buoyancy effect. On the other hand, a heat sink in the boundary layer absorbs energy, causing the fluid temperature to decrease, which in turn reduces the flow velocity in the boundary layer as a result of the buoyancy effect.

4. Conclusion

Steady, laminar, viscous boundary layer flow over an accelerating semi infinite porous surface in the presence of a magnetic field, thermal radiation, buoyancy, heat generation or absorption was considered. The coupled nonlinear partial differential equations were solved numerically by the perturbation technique. The results for a simplified case with no radiation and no magnetic field were compared with the previous works and to be found in a good agreement. Next calculations were performed for a more general case and find out that the wall heat transfer decreases in the presence of magnetic field, heat generation, thermal radiation or positive wall mass transfer, while it increases due to the thermal buoyancy forces.

Acknowledgements

Appreciation is extended to the referees for their constructive and helpful comments and suggestions. These led to improvements in the revised paper.

APPENDIX

$$a_1 = \frac{\left(\frac{AP_r}{N_R+1}\right) + \sqrt{\left(\frac{AP_r}{N_R+1}\right)^2 - 4\left(\frac{\Delta P_r}{N_R+1}\right)}}{2},$$

$$a_2 = \frac{-A - \sqrt{A^2 + 4M^2}}{2},$$

$$a_3 = \frac{(a_1^2 - Aa_1 - M^2) + G_r}{a_2(a_1^2 - Aa_1 - M^2)},$$

$$a_5 = \frac{(1+\delta_x)a_3a_2 + a_1a_3}{\left((a_2 - a_1)\left(\frac{N_R+1}{P_r}(a_2 - a_1) + A\right) + \Delta\right)},$$

$$a_6 = \frac{-\delta_x G_r}{(a_1^2 - Aa_1 - M^2)\left(\frac{4a_1^2(N_R+1)}{P_r} - 2Aa_1 + \Delta\right)},$$

$$a_7 = \frac{-\left(a_1f_0 + a_1a_3 + \frac{G_r}{(a_1^2 - Aa_1 - M^2)}\right)}{\left(\frac{AP_r}{(N_R+1)} - 2a_1\right)},$$

$$a_8 = -a_3a_2\left(a_2f_0 + a_3a_2 + \frac{a_2G_r}{a_1(a_1^2 - Aa_1 - M^2)}\right),$$

$$a_9 = \frac{-G_r}{(a_1^2 - Aa_1 - M^2)}\left(a_1f_0 + a_3a_1 + \frac{G_r}{(a_1^2 - Aa_1 - M^2)}\right),$$

$$a_{10} = \frac{G_r^2}{(a_1^2 - Aa_1 - M^2)},$$

$$a_{11} = \frac{a_3G_r(a_1^2 + a_2^2)}{a_1(a_1^2 - Aa_1 - M^2)},$$

$$a_{12} = \frac{2a_2a_{13}G_r}{(a_1^2 - Aa_1 - M^2)},$$

$$a_{13} = \frac{(a_5 + a_6)G_r}{a_1(a_1^2 - Aa_1 - M^2)},$$

$$a_{14} = \frac{(a_5G_r + a_{11} + a_{12})}{(a_2 - a_1)((a_2 - a_1)^2 + A(a_2 - a_1) - M^2)},$$

$$a_{15} = \frac{G_ra_6}{2a_1(4a_1^2 - 2a_1A - M^2)},$$

$$a_{16} = \frac{a_9}{a_1(a_1^2\ a_1A - M^2)},$$

$$a_{17} = (-a_1a_{13} + a_{14}(a_2 - a_1) + 2a_1a_{15} + a_1a_{16} - a_{92} - a_{93} + a_1a_{94})/a_2,$$

$$a_{18} = -a_{17} + a_{13} + a_{14} - a_{15} - a_{16} - a_{94},$$

$$a_{92} = \frac{-a_8}{3a_2^2 + 2Aa_2 - M^2},$$

$$a_{93} = \frac{a_7G_r}{a_1(a_1^2 - Aa_1 - M^2)},$$

$$a_{94} = \frac{a_{93}(3a_1^2 - 2Aa_1 - M^2)}{(a_1^2 - Aa_1 - M^2)}$$

REFERENCES

[1] J.A. Shercliff. *A text book of Magnetohydrodynamic*. Pergamon Press, 1965.

[2] P.C. Ram, S.S. Singh, R.K. Jain. Heat and mass transfer of a viscous heat generating fluid with Hall currents. *AstroPhys. Space Sci.*, **168**: 209, 1990.

[3] B.K. Jha, R. Prasad. MHD free convection and mass transfer flow through a porous medium with heat source. *AstroPhys. Space Sci.*, **181**(1): 117, 1991.

[4] H.S. Takhar, P.C. Ram, E.J.D. Garba, J.K. Bitok. Hydromagnetic convective flow of heat generating fluid past a vertical plate with Hall current and heat flux through a porous medium. *J. MHD Plasma Res.*, **5**(2/3): 185, 1995.

[5] D.P. Georgiou, G.A. Georgantopoulos. Mass transfer effects on the transient behaviour of the asymptotic laminar boundary layer, *AstroPhys. Space Sci.*, **125**: 391, 1986.

[6] V.M. Soundalgekar, J.P. Bhat, M. Miuddin. Finite difference analysis of free convection effects on Stokes problem for a vertical plate in a dissipative fluid with constant heat flux. *J. Heat Mass Transfer*, **9**: 199, 1985.

[7] P.C. Ram. Finite difference analysis of the MHD Stokes problem for a vertical plate with Hall and ion-slip currents. *AstroPhys. Space Sci.*, **176**: 263, 1991.

[8] N. Chaturuedi. The flow of incompressible viscous fluid past an impulsively started infinite porous plate with variable suction. *Energy Convers. Mgmt.*, **38**: 1699, 2000.

[9] K. Vajravelu, A. Hadjinicolaou. Convective heat transfer in an electrically conducting fluid at a stretching surface with uniform free stream. *Int. J. Engng. Sci.*, **35**(12/13), 1237, 1997.

[10] T.C. Chiam. Hydromagnetic flow over a surface stretching with a power low velocity. *Int. J. Engng. Sci.*, **33**: 429, 1995.

[11] I. Pop., T.Y. Na. A note on MHD flow over a stretching permeable surface. *Mech. Res. Commun.*, **25**: 263, 1998.

[12] A.J. Chamkha. Thermal radiation and buoyancy effects on hydromagnetic flow over an accelerating permeable surface with heat source or sink. *Int. J. Engng. Sci.*, **38**: 1699, 2000.

[13] M.M. Abdelkhalek. Two phase flow in a two dimensional horizontal channel. *Al-Azhar Engineering Fifth International Conference*, Vol. 8, pp.31–42,Dec. 19–22, 1997.

[14] M.M. Abdelkhalek. Numerical simulation of the motion of charged suspended particle in multi-phase flow. *Egypt. J. Phys.*, **29**(1): 39, 1998.

[15] M.M. Abdelkhalek, M.N.H. Comsan. Numerical simulation of multiphase flow in a channel. *Egypt. J. Phys.*, **30**(1): 107, 1999.

[16] M.M. Abdelkhalek. Free convection along a vertical plate with variable surface temperature. *Arab J. Nucl. Sci. Appl.*, **36**(2): 179, 2003.

[17] M.M. Abdelkhalek. Hydromagnetic free convection flow past a uniformly accelerated plate". *Arab J. Nucl. Sci. Appl.*, **36**(2): 189, 2003.

[18] M.M. Abdelkhalek. Mathematical analysis of the effects of mass transfer on an oscillating free convection flow. *Egypt. J. Phys.*, **34**(2): 267, 2003.

[19] M.M. Abdelkhalek. Influence of a magnetic field and axisymmetric flow near a stagnation point. *Arab J. Nucl. Sci. Appl.*, **37**(1): 257–267, 2004.

[20] M.M. Abdelkhalek. Mathematical analysis for hydromagnetic flow with free convection and mass transfer along a vertical infinite porous plate. *Proceedings of the International Conference on Mathematics Nuclear Physics and Applications in the 21 Century*, 479, Cairo, March 8-13, 2003.

[21] H.S. Takhar, R.S.R. Gorla, V.M. Soundalgekar. Radiation effect on MHD free convection flow of a gas past a semi- infinite vertical plate. *Int. Num. Math. Heat Fluid Flow*, **77**, 1996.

[22] E.M.A. Elbashbeshy. Radiation effect on heat transfer over a stretching surface. *Can. J. Phys.*, **78**: 1107, 2000.

[23] M. Acharya, L.P. Singh, G.C. Dash. Heat and mass transfer over an accelerating surface with heat source in presence of suction and blowing. *Int. J. Engng. Sci.*, **37**: 189, 1999.

[24] A. Raptis. Flow of a micropolar fluid past a continuously moving plate by the presence of radiation. *Int. J. Heat Mass Transfer*, **41**: 2865, 1998.

[25] E.M. Sparrow, D.R. Cess. *Radiation Heat Transfer*, Augmented Edition (Chapters 7 and 10, 19). Hemisphere Publishers, Washington, DC, 1978.

[26] K. Vajravelu, J. Nayfeh. Hydromagnetic convection at a cone and a wedge. *Int. Commun. Heat Mass Transfer*, **19**: 701, 1992.

[27] A.J. Chamkha. Non-Darcy hydromagnetic free convection from a cone and a wedge in porous media. *Int. Commun. Heat Mass Transfer*, **23**: 875, 1996.